

Poisson's ratios ν_i appearing in Eqs. (11–18) are given by

$$[D_{xx}; D_{\theta\theta}; D_{x\theta}] = \sum_{i=1}^n t_i r_i^2 [K_{11}^i; K_{22}^i; K_{33}^i] \quad (19)$$

$$[C_{xx}; C_{\theta\theta}; C_{x\theta}] = \sum_{i=1}^n t_i r_i [K_{11}^i; K_{22}^i; K_{33}^i] \quad (20)$$

$$[B_{xx}; B_{\theta\theta}; B_{x\theta}] = \sum_{i=1}^n t_i [K_{11}^i; K_{22}^i; K_{33}^i] \quad (21)$$

$$[D_{xx}; D_{\theta z}] = \sum_{i=1}^m h_i [K_{44}^i; K_{55}^i] \quad (22)$$

$$\begin{aligned} \nu_1 &= \frac{1}{D_{xx}} \sum_{i=1}^n t_i r_i^2 K_{12}^i; & \nu_2 &= \frac{1}{C_{xx}} \sum_{i=1}^n t_i r_i K_{12}^i \\ \nu_3 &= \frac{1}{D_{\theta\theta}} \sum_{i=1}^n t_i r_i^2 K_{22}^i; & \nu_4 &= \frac{1}{C_{\theta\theta}} \sum_{i=1}^n t_i r_i K_{12}^i \\ \nu_5 &= \frac{1}{B_{xx}} \sum_{i=1}^n t_i K_{12}^i; & \nu_6 &= \frac{1}{B_{\theta\theta}} \sum_{i=1}^n t_i K_{12}^i \end{aligned} \quad (23)$$

Equations (19, 21, and 22) give the multilayer sandwich shell stiffness in bending, extension, and shear, respectively. Equation (20) defines the coupling stiffnesses of the shell. Equation (22) gives the transverse shearing stiffnesses; and Eq. (23) defines the modified Poisson's ratio of the shell.

References

- ¹ Liaw, B. D. and Little, R. W., "Theory of Bending Multilayer Sandwich Plates," *AIAA Journal*, Vol. 5, No. 2, Feb. 1967, pp. 301–304.
- ² Azar, J. J., "Bending Theory for Multilayer Orthotropic Sandwich Plates," *AIAA Journal*, Vol. 6, No. 11, Nov. 1968, pp. 2166–2169.
- ³ Wong, J. P. and Salama, A. B., "Stability of Multilayer Sandwich Plates," Rept. 93 (EM 3), 1967, Structural Div., American Society of Civil Engineers, pp. 19–31.
- ⁴ Donnell, L. E., "Stability of Thin-Walled Tubes Under Torsion," TR 2017, 1950, NACA.

Boundary-Layer Induced Pressures on a Flat Plate in Unsteady Hypersonic Flight

TSE-FOU ZIEN* AND ELI RESHOTKO†

Case Western Reserve University, Cleveland, Ohio

Introduction

IN this Note a procedure is developed for the calculation of hypersonic viscous interaction pressures for unsteady flows, valid for weak interactions. This procedure is based on an extension of the idea underlying the tangent wedge approximation which is generally accepted for the calculation of interaction pressures in steady flows. Examples are then worked out, using this method, to illustrate the unsteady features of the interaction pressures. The simple, yet non-trivial, flow configuration of a semi-infinite flat plate moving in its own plane with various situations of motion unsteadiness is chosen to demonstrate the idea, and use is made of

the available solutions for such unsteady boundary-layer flows without interactions. Results are reported for the first approximation of weak interaction pressures for the unsteady situations considered. For this class of flow geometry it is obvious that the effects of flow unsteadiness on the aerodynamic forces do not appear in an inviscid analysis. It is believed that the present study is useful for the determination of various aerodynamic forces on hypersonic vehicles in unsteady flight, and that the results reported here are new. Many details of the analysis and calculations are omitted in this Note but appear in Ref. 1.

Analysis

Let the displacement surface of an unsteady boundary layer with no interaction be denoted by

$$F(x, y, t) \equiv y - \Delta(x, t) = 0 \quad (1)$$

where the rectangular Cartesian coordinate system (x, y) is fixed with respect to the plate, with its origin at the leading edge of the plate. The plate is moving with a continuously varying (otherwise arbitrary) velocity, $U(t)$, in the negative x direction. Then the first approximation of the weak interaction pressure on such a plate is just the pressure on the two-dimensional unsteady surface $y = \Delta(x, t)$, which moves in the negative x direction at a hypersonic Mach number, $M(t) = U(t)/a_\infty \gg 1$, a_∞ being the ambient sound speed.

To proceed, we shall first indicate how the "weak" form of the tangent wedge approximation used in Ref. 2 to calculate weak interaction pressures for steady flows can be extended and employed for the present unsteady flows.

We note that the tangent wedge formula in its normal form corresponds to the leading approximation to the exact solution of supersonic wedge flow in the limit of $\theta_b \rightarrow 0$, $M_\infty \rightarrow \infty$ with $K_b \equiv M_\infty \theta_b$ fixed, where θ_b is to be taken as the local body inclination angle with the freestream and M_∞ is the freestream Mach number, U/a_∞ . The surface pressure thus obtained is the same as that on a one-dimensional piston pushing into still air with a velocity equal to $U\theta_b$, the approximate normal velocity of the surface at the local point under consideration. The weak form of the tangent wedge approximation, which corresponds to the limit $\theta_b \rightarrow 0$, $M_\infty \rightarrow \infty$ with $K_b \rightarrow 0$, is thus equivalent to the further approximation of low piston Mach number, i.e., $U\theta_b/a_\infty \ll 1$, in the one-dimensional piston problem.

By relating the results of tangent wedge approximation to those of the one-dimensional piston problem as in the aforementioned, the idea of the tangent wedge approximation can be easily extended to unsteady flows by simply regarding the surface element as a piston moving with a time dependent speed equal to the normal velocity of the unsteadily moving surface at the particular point concerned. In particular, the first approximation of the surface pressure for unsteady, weak interactions can thus be taken to be the acoustic pressure on a piston moving at a variable, but low, speed.

It may be worth mentioning here that, by following this reasoning, it is possible to extend the "strong" form of the tangent wedge approximation used in Ref. 2 to calculate the steady strong interaction pressures to handle the unsteady strong interaction problems. Here we have the situation of $K_b \gg 1$, which corresponds to the case of a piston pushing with a very high (time dependent) Mach number into air at rest. Then the so called "snowplow theory," for example, might be one of the possibilities for providing a relationship

Table 1 Values of k , k_0 , and k_1

	Insulated	Isothermal
k	0.56	0.14
k_0	-2.83	-0.23
k_1	5.10	0.33

Received May 14, 1969; revision received September 25, 1969. This work was supported by the Air Force Office of Scientific Research under Grant AFOSR 68-1581.

* Research Associate, Division of Fluid, Thermal and Aerospace Sciences.

† Professor of Engineering.

between the pressure distribution and the surface geometry. Of course, it must be remembered that in dealing with strong interaction problems the displacement surface must be calculated taking into account the induced pressure field. Further discussion on the subject of unsteady strong interactions will not be pursued here.

The next step then is to determine the "piston speed," i.e., the normal velocity, q_n , of an element on the moving surface defined by Eq. (1). This is a straightforward calculation involving only the application of the inviscid velocity boundary condition on the surface. The result is (see Ref. 1 for details), for $(\partial\Delta/\partial x)^2 \ll 1$,

$$q_n = \partial\Delta/\partial t + U(t)\partial\Delta/\partial x \quad (2)$$

With the "piston speed," q_n , so determined, the pressure on the piston, P_b , can be approximated as

$$(P_b - P_\infty)/P_\infty = \gamma q_n/a_\infty + O(q_n/a_\infty)^2 \quad (3)$$

The leading term represents the result of acoustic theory, and P_∞ and γ denote the ambient static pressure and the ratio of the specific heats, respectively, both being constants.

It remains to find an expression for $\Delta(x, t)$ in terms of the boundary-layer solutions which are presumed to be known. The displacement surface of a general three-dimensional, unsteady boundary layer over an impermeable surface was discussed by Moore and Ostrach.³ They obtained an equation for Δ , which reduces in the flow situations under our consideration to the following simple form:

$$U\partial\Delta/\partial x + \partial\Delta/\partial t = U\partial\delta^*/\partial x + \partial\delta_\rho/\partial t \quad (4)$$

with

$$\delta^*(x, t) \equiv \int_0^\infty \left(1 - \frac{\rho u}{\rho_\infty U}\right) dy \quad (5a)$$

and

$$\delta_\rho(x, t) \equiv \int_0^\infty \left(1 - \frac{\rho}{\rho_\infty}\right) dy \quad (5b)$$

In Eqs. (5), ρ and u denote the boundary-layer solutions of density and velocity fields, respectively.

Combining Eqs. (2, 3, and 4) we have an expression for the first approximation of the weak interaction pressures on the plate in terms of the boundary-layer solutions in the absence of interactions. It is

$$(P_b - P_\infty)/P_\infty = \gamma[M(t)\partial\delta^*/\partial x + (1/a_\infty)\partial\delta_\rho/\partial t] + \dots \quad (6)$$

where P_b is the static pressure on the plate. Equation (6) will be applied in the following section to various situations of unsteady motions where the boundary-layer solutions are available.

Examples and Discussions

The following two cases of unsteady motions will be considered and the corresponding interaction pressures will be obtained through the use of Eq. (6). The results are all based on the assumptions of a linear variation of viscosity with temperature (i.e., $\rho\mu = c\rho_\infty\mu_\infty$) and a constant Prandtl number, Pr , of 0.72.

Nearly quasi-steady flows

The boundary-layer solutions due to Moore⁴ and Ostrach⁵ are employed and the induced pressures are found, after some calculations, to have the following form:

$$\frac{P_b - P_\infty}{P_\infty} = \frac{\gamma(\gamma - 1)}{(R)^{1/2}} M^3(k + k_0\zeta_0 + k_1\zeta_1 + \dots) \quad (7)$$

where R is the Reynolds number defined by $U(t)x/\nu$, ν being

Table 2 Values of λ and ϕ

	Insulated plate	Isothermal plate
λ	$2.5(1 - 1.61\Omega^2) + O(\Omega^4)$	$2.5(1 - 0.72\Omega^2) + O(\Omega^4)$
ϕ	$\tan^{-1}[2.03\Omega + O(\Omega^3)]$	$\tan^{-1}[0.64\Omega + O(\Omega^3)]$

the scaled kinematic viscosity ($\equiv c\mu_\infty/\rho_\infty$), ζ_0, ζ_1, \dots are a sequence of parameters which characterize flow unsteadiness, and they are defined as

$$\zeta_0 \equiv xU'(t)/U^2, \zeta_1 \equiv x^2U''(t)/U^3 \text{ etc.}$$

These parameters form a diminishing sequence in the limit of small flow unsteadiness. The constants, k 's, are given in Table 1.

We note here that the preceding results are based on the approximation of very high Mach numbers, i.e., $M^2(t) \gg 1$ and $(\theta_w - \theta_\infty)/\theta_\infty$ (the temperature parameter in the case of isothermal plate). Also to be noted is that the values of k agree with those for steady flows as given in Ref. 2.

It is obvious from Eq. (7) that the principal parameter for the interaction pressure, $M^2/(R)^{1/2}$, enters the unsteady flows with the same form, but is now a function of t as well as x . Also to be noted is the fact that the contribution of the term $\partial\delta_\rho/\partial t$ to the terms associated with ζ_0, ζ_1 , etc. in the preceding results is of the same order as that of the term $\partial\delta^*/\partial x$.

The fact that k_0 is negative for both insulated and isothermal plates clearly indicates that an acceleration tends to decrease the induced pressure. This is evidently a consequence of the fact that the influence of the viscous boundary layer on the external inviscid field is reduced by the strong "thinning effect" on the boundary layer due to accelerations.

A particular example of a plate executing small oscillation about a mean velocity will then be worked out using the preceding general results. We let

$$U(t) = u_0(1 + \epsilon \sin \omega t) \quad (8)$$

with $M_0 (\equiv u_0/a_\infty) \gg 1$. A frequency parameter, $\Omega (\equiv x\omega/u_0)$, is assumed to be small in order for the preceding results to apply. The small parameters ϵ and Ω are ordered in such a way that

$$\epsilon \ll \Omega \ll 1$$

The induced pressures are obtained as follows:

$$(P_b - P_\infty)/P_\infty = k\gamma(\gamma - 1)[M_0^3/(R_0)^{1/2}] \times [1 + \epsilon\lambda \sin(\omega t - \phi) + O(\epsilon^2)] \quad (9)$$

where $R_0 \equiv u_0x/\nu$ and the quantities λ and ϕ are shown in Table 2.

It is noted here that in the preceding calculations, the contribution to the leading approximation of the phase difference comes solely from the ζ_0 term, whereas the contribution to the amplitude variation λ , results from both ζ_0 and ζ_1 terms. The phase of the induced pressures is always lagging behind that of the plate velocity by a quantity of order Ω . For the practical application of the preceding results, Ω must be sufficiently small, say smaller than $\frac{1}{3}$, so that the deviation of the amplitude from its steady value is small.

These results also indicate that for both insulated and isothermal plates, the amplitude of the induced pressure decreases with increasing Ω , while the phase lag of the induced pressure increases with increasing Ω .

Initial stage of motion

In this limit the boundary-layer solution is expected to be independent of x because the existence of the leading edge has not yet been felt by the downstream stations. Obviously, the results also apply to the case of a doubly infinite flat plate. The special class of flows with

$$U(t) = At^m$$

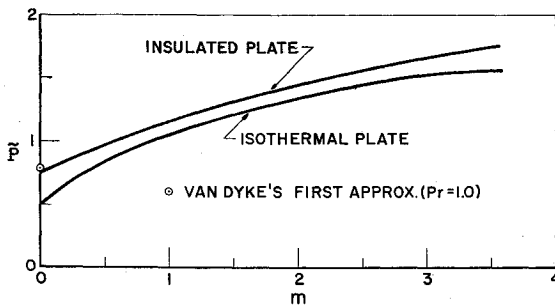


Fig. 1 Induced pressures for the initial stage case, with $U(t) = At^m$;

$$\bar{P} \equiv \left(\frac{P_b}{P_\infty} - 1 \right) / \left[\frac{\gamma(\gamma-1)}{2} M^2 R^{-1/2} * \right]$$

will be studied, using the results of the boundary-layer solutions recently reported by Yang and Huang.⁶ Note here that in applying Eq. (6), only δ_0 is relevant. This implies that the induced pressure in this case results solely from density defects inside a boundary layer. The induced pressures have the following form:

$$(P_b - P_\infty)/P_\infty = [\gamma(\gamma-1)/2](\frac{1}{2} + m)K(m)M^2/(R^*)^{1/2} \sim t^{(2m-1/2)} \quad (10)$$

where $R^* \equiv a_\infty^2 t/\nu$ and $K(m)$ is a known constant, with different values for insulated and isothermal plates, for each given value of m . Results of Eq. (10) are illustrated in Fig. 1.[†]

We note here that the form of the induced pressure in this limit is the same as that given by Van Dyke⁷ who treated a case equivalent to $m = 0$ in our results but with $Pr = 1$. Also it is interesting to note that $m = \frac{1}{4}$ is a distinguished case for which the induced pressure, to first approximation, is constant in time.

In conclusion, we remark that the unsteady, weak interaction pressures on a flat plate have been worked out for both the case of small flow unsteadiness and the case of initial stages of motion (or equivalently, the case of a doubly infinite flat plate). It has also been indicated that the idea based on which the method of calculations reported in this Note is developed may probably be employed to pursue the study of the conceivably more complex problem of strong pressure interactions in unsteady flows.

References

- ¹ Zien, T. F. and Reshotko, E., "Boundary Layer Induced Pressures on a Flat Plate in Unsteady Hypersonic Flight," AFOSR Scientific Report 69-1229TR, May 1969, Case Western Reserve Univ.
- ² Hayes, W. D. and Probstein, R. F., *Hypersonic Flow Theory*, 1st ed., Academic Press, New York, 1959, Chap. 9.
- ³ Moore, F. K. and Ostrach, S., "Displacement Thickness of the Unsteady Boundary Layers," *Journal of the Aerospace Sciences*, Vol. 24, 1957, pp. 77-78.
- ⁴ Moore, F. K., "Unsteady Laminar Boundary Layer Flow," TN2471, 1951, NACA.
- ⁵ Ostrach, S., "Compressible Laminar Boundary Layer and Heat Transfer for Unsteady Motions of a Flat Plate," TN3569, 1955, NACA.
- ⁶ Yang, W. J. and Huang, H. S., "Unsteady Compressible Laminar Boundary-Layer Flow over a Flat Plate," *AIAA Journal*, Vol. 7, No. 1, Jan. 1969, pp. 100-105.
- ⁷ Van Dyke, M. D., "Impulsive Motion of an Infinite Plate in a Viscous Compressible Fluid," *Zeitschrift fuer Angewandte Mathematik und Physik*, Vol. 3, 1952, pp. 343-353.

[†] Errors in the numerical values of Table 1 in Ref. 6 have been noticed, and corrected values were obtained through private communications.

Experimental Verification of St. Venant's Principle in a Sandwich Beam

R. S. ALWAR*

Indian Institute of Technology, Madras, India

ST. VENANT'S principle is well known and has been demonstrated theoretically and also experimentally. From this principle it is understood that the difference between the stresses caused by two statically equivalent load systems is insignificant at and beyond a distance equal to the largest linear dimension of the area over which these load systems are applied. But it has also been shown in some cases such as thin walled structures¹ and space trusses² that a self-equilibrating load induces significant stresses even at large distances from the end. In other words, in such cases the effect of replacing one load system by another statically equivalent load system is felt significantly at large distances beyond the area of application of the load.

In this Note one such case, namely the problem of a sandwich beam subjected to two different statically equivalent load systems, has been investigated, and it has been shown that the difference between the stresses caused by these two statically equivalent load systems at a distance equal to the depth of the beam and beyond is much larger than what it would be in the case of a homogeneous beam.[†] Also it is shown that this is true only under a certain condition, viz., when the Young's modulus of the core is quite small compared to the Young's modulus of the face layers. The author, attempting to give exact solutions by elasticity theory to sandwich plates, found it necessary to use the St. Venant's principle in order to satisfy the boundary conditions at the thickness edge of the plate. In this connection, it was thought worthwhile to investigate how valid this principle is in the case of a sandwich beam. It can also be mentioned that this principle is assumed or used indirectly in many cases connected with analysis of sandwich structures. A better understanding of this problem will lead to a more judicious application of this principle in the field of sandwich structural analysis.

As a first step in this process, experiments were carried out on a simple sandwich cantilever beam using a photoelastic technique. The sandwich beams were 25 cm long and 5 cm deep. The depth of each of the layers was 2 cm and the depth of the core was 1 cm. The width of the beam was 1.5 cm. In order to prevent the lateral buckling of the low modulus core it was necessary to keep the width of the beam considerably large, although this introduced additional difficulties in accurate measurement of the fringe order at the

Table 1 Model materials

Case 1	Face layers	Araldit D (epoxy resin)
	core layer	Silicone Kautschuk Gießmasse (rubber)
Case 2	Face layers	Araldit D
	core layer	Araldit D + 45% Thiokol (plasticizer)
Case 3	Homogeneous beam	

Received June 2, 1969; revision received August 22, 1969. The author is deeply indebted to H. Neuber and E. Mönch for providing the opportunity to work in the photoelastic Laboratory of Technische Hochschule München, where these investigations were conducted. Thanks are also due to H. Ficker for providing the necessary facilities.

* Assistant Professor, Department of Applied Mechanics.

[†] It is possible that one can arrive at this conclusion with certain amount of reasoning. But the object of this investigation is to give a quantitative estimate of this effect.